Shape sensitivity calculations for exterior acoustics problems

Gonzalo R. Feijóo, Manish Malhotra, Assad A. Oberai and Peter M. Pinsky
Division of Mechanics and Computation, Stanford University, California, USA

Keywords *Shape optimization, Acoustics, Sensitivity evaluation, Inverse problems*

Abstract *The purpose of this paper is to present a method to calculate the derivative of a functional that depends on the shape of an object. This functional depends on the solution of a linear acoustic problem posed in an unbounded domain. We rewrite this problem in terms of another one posed in a bounded domain using the Dirichlet-to-Neumann (DtN) map or the modified DtN map. Using a classical method in shape sensitivity analysis, called the adjoint method, we are able to calculate the derivative of the functional using the solution of an auxiliary problem. This method is particularly efficient because the cost of calculating the derivatives is independent of the number of parameters used to approximate the shape of the domain. The resulting variational problems are discretized using the finite-element method and solved using an efficient Krylov-subspace iterative scheme. Numerical examples that illustrate the efficacy of our approach are presented.*

1. Introduction

In this study we consider the problem of calculating derivatives of shape functionals, i.e. functionals that depend on the shape of an object, with constraints given by the scalar Helmholtz equation posed in an unbounded domain. These derivatives are needed in several problems, including shape optimization and inverse problems. The main purpose of this paper is to describe a procedure to efficiently calculate these derivatives.

One method that is widely used in the shape sensitivity literature is the adjoint method. This procedure allows us to calculate the derivative of a functional with constraints, for any direction of change of the variables, by solving an auxiliary problem, called the adjoint problem. In this work we extend this method to include the case where the constraints are given by the equations of exterior acoustics, and therefore when the solution of the constraint equations is a complex-valued scalar field.

This paper is organized as follows. In Section 2, we briefly review the exterior Helmholtz problem and its variational formulation. The problem is

Manish Melhotra is currently with Sun Microsystems, Palo Alto, California, USA.

This work was supported by ONR under contract N00014-99-1-0121 with Stanford University. Computational resources for our calculations were provided by a generous gift from Intel Corporation. Gonzalo R. Feijóo was partially supported by Brazilian government fellowship from CNPq 200895/94-0. The support from all these agencies and companies is greatly appreciated.

Engineering Computations,
Vol. 18 No. 3/4, 2001, pp. 376-391.

posed in terms of a bounded domain by using the Dirichlet-to-Neumann (DtN) boundary condition (Keller and Givoli, 1989). In section 3, we show how to calculate derivatives of shape functionals by defining a change in shape through a mapping defined over an original configuration. We then define a Lagrangian functional which allows us to calculate the shape derivative by solving an adjoint problem. In section 4, we consider the numerical approximation aspects of this calculation. In section 5, we consider two numerical examples, and we present our conclusions in section 6.

2. The exterior Helmholtz problem

The exterior Helmholtz problem in d dimensions posed on the unbounded domain $\Omega_\infty \subset \mathbb{R}^d$ (see Figure 1) is given as follows: find u such that:

$$-\nabla^2 u - k^2 u = f \quad \text{in } \Omega_\infty = \Omega_{\text{ext}} \cup \Omega, \tag{1}$$

$$u = g \quad \text{on } \Gamma_g, \tag{2}$$

$$\nabla u \cdot \boldsymbol{n} = h \quad \text{on } \Gamma_h \tag{3}$$

$$\lim_{r\to\infty} r^{(d-1)/2}\left(\frac{\partial u}{\partial r} - iku\right) = 0, \tag{4}$$

where k is the wave number, f is a prescribed external force, g is a prescribed Dirichlet boundary condition, h is a prescribed Neumann boundary condition and equation (4) is the Sommerfeld boundary condition, which is imposed at infinity.

The problem given by equations (1)-(4) can be equivalently posed on a bounded domain where the condition imposed at the truncating surface incorporates the effect of the unbounded domain. This is accomplished via the DtN or the modified DtN map (Oberai *et al.*, 1998). The corresponding boundary-value problems are given by: find u such that:

$$-\nabla^2 u - k^2 u = f \quad \text{in } \Omega, \tag{5}$$

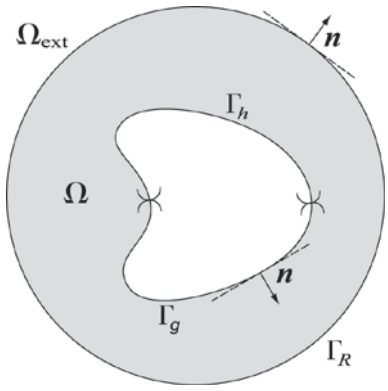

Figure 1.
Domain definitions for the exterior acoustics problem

$$u = g \quad \text{on } \Gamma_g, \tag{6}$$

$$\nabla u \cdot \boldsymbol{n} = h \quad \text{on } \Gamma_h, \tag{7}$$

$$\nabla u \cdot \boldsymbol{n} = M(u) \quad \text{on } \Gamma_R, \tag{8}$$

where (8) is the non-reflecting boundary condition imposed at Γ_R. In both formulations, the operator $M(u)$ can be represented as follows:

$$M(u) = B(u) + \sum_{n=N(d)}^{\infty} \sum_{j=-J(d)}^{J(d)} \hat{z}_{|n|}(k, R; d)\psi_{nj}(\boldsymbol{x}; d) \int_{\Gamma_R} \psi_{nj}^*(\boldsymbol{x}_0; d)u(\boldsymbol{x}_0)d\Gamma_0, \tag{9}$$

where an asterisk denotes the complex conjugate of a quantity, $B(u)$ is a linear operator and

$$N(d) = \begin{cases} -\infty & d = 2 \\ 0 & d = 3 \end{cases}, \tag{10}$$

$$J(d) = \begin{cases} 0 & d = 2 \\ n & d = 3 \end{cases}, \tag{11}$$

$$\psi_{nj}(\boldsymbol{x}; d) = \begin{cases} \sqrt{\frac{1}{2\pi R}} \exp(\mathrm{i}n\theta) & d = 2 \\ \sqrt{\frac{(2n+1)(n-|j|)!}{4\pi R^2(n+|j|)!}} P_n^{|j|}(\cos\theta)\exp(\mathrm{i}j\phi) & d = 3 \end{cases}, \tag{12}$$

$P_{|n|}^{j}$ is the associated Legendre polynomial of degree n and order j, $d\Gamma_0$ is the differential element corresponding to Γ_R. Γ_R is a ball of radius R that encloses the object. The impedance coefficients $\hat{z}_{|n|}(k, R; d)$ and the local operator $B(u)$ depend on the formulation and are given by the following:

- For the DtN map

$$B(u) = 0, \tag{13}$$

$$\hat{z}_{|n|}(k, R; d) = z_{|n|}(k, R; d) = \begin{cases} \frac{kH_n^{(1)'}(kR)}{H_n^{(1)}(kR)} & d = 2 \\ \frac{kh_n^{(1)'}(kR)}{h_n^{(1)}(kR)} & d = 3 \end{cases}, \tag{14}$$

- For the modified DtN map

$$B(u) = \alpha(k, R; d)u(R, \boldsymbol{x}), \tag{15}$$

$$\hat{z}_{|n|}(k, R; d) = z_{|n|}(k, R; d) - \alpha(k, R; d), \tag{16}$$

$$\alpha(k,R;d) = \begin{cases} \mathrm{i}k - \frac{1}{2R} & d = 2 \\ \mathrm{i}k - \frac{1}{R} & d = 3 \end{cases}. \tag{17}$$

In the above expressions, $H^{(1)}_{|n|}$ is the Hankel function of the first kind of order n and $h^{(1)}_{|n|}$ is the spherical Hankel function of the first kind of order n.

The weak form associated with the boundary-value problem (5)-(8) is given by: find $u \in \mathcal{S}_\Omega$ such that:

$$a(\Omega; w, u) = \ell(\Omega; w) \qquad \forall w \in \mathcal{V}_\Omega, \tag{18}$$

where

$$a(\Omega; w, u) = (\nabla w, \nabla u)_\Omega - k^2 (w, u)_\Omega - (w, M(u))_{\Gamma_R}, \tag{19}$$

$$\ell(\Omega; w) = (w, f)_\Omega + (w, h)_{\Gamma_h}. \tag{20}$$

The inner products in (19) and (20) are defined by:

$$(w, u)_\Omega = \int_\Omega w^* u \, d\Omega, \tag{21}$$

$$(w, u)_{\Gamma_R} = \int_{\Gamma_R} w^* u \, d\Gamma, \tag{22}$$

$$(w, h)_{\Gamma_h} = \int_{\Gamma_h} w^* u \, d\Gamma, \tag{23}$$

and the set $\mathcal{S}_\Omega$ and the linear space $\mathcal{V}_\Omega$ by:

$$\mathcal{S}_\Omega = \{u \in H^1(\Omega);\ u(\boldsymbol{x}) = g(\boldsymbol{x}),\ x \in \Gamma_g\}, \tag{24}$$

$$\mathcal{V}_\Omega = \{u \in H^1(\Omega);\ u(\boldsymbol{x}) = 0, x \in \Gamma_g\}. \tag{25}$$

3. Calculation of shape sensitivities

We now consider a generic cost functional which depends on Ω:

$$j(\Omega) = J(\Omega, u(\Omega)) \tag{26}$$

where the scalar field u, also called the primal field, satisfies the variational problem given by (18), also called the state equation. Written in this form, the functional $J(\Omega,\ u(\Omega))$ depends on the shape of the domain both explicitly (through its first argument) and implicitly (through the primal field which depends on Ω). We want to calculate the derivative of $j(\Omega)$ with respect to

changes in the domain Ω. This derivative is called the shape derivative. In order to perform this calculation, we study the behavior of the functional with respect to changes in the domain Ω through a uniparametric family of transformations $\phi_\varepsilon = \phi_\varepsilon(\boldsymbol{V})$ such that for a given $\boldsymbol{x} \in \Omega$ we have $\phi_\varepsilon(\boldsymbol{V})(\boldsymbol{x}) = \boldsymbol{x}_\varepsilon$, where

$$\boldsymbol{x}_\varepsilon = \boldsymbol{x} + \varepsilon \boldsymbol{V}(\boldsymbol{x}), \tag{27}$$

$\varepsilon \in \mathbb{R}$, and $\boldsymbol{V}$ is a given smooth vector field in $\mathbb{R}^d$ called the direction of change of the domain. We note that by using the transformation (27) we are characterizing shape changes with changes in the parameter ε and therefore the differentiation with respect to shape is recast to a well-known operation, differentiation with respect to a scalar. We also say that by means of the mapping (27) the domain Ω is mapped to the domain Ω_ε, and write $\Omega_\varepsilon = \phi_\varepsilon(\Omega)$ where

$$\Omega_\varepsilon = \{\boldsymbol{x}_\epsilon | \boldsymbol{x}_\varepsilon = \boldsymbol{x} + \varepsilon \boldsymbol{V}(\boldsymbol{x}), \boldsymbol{x} \in \Omega\}. \tag{28}$$

This idea, originally proposed by Hadamard (1968), allows us to make use of standard results in continuum mechanics to evaluate the shape derivative by rewriting all the functional terms with respect to a fixed configuration Ω.

From the discussion above we define the derivative of the functional $j(\Omega)$ with respect to the domain Ω in the $\boldsymbol{V}$ direction, denoted $Dj(\Omega) \cdot \boldsymbol{V}$, by:

$$Dj(\Omega) \cdot \boldsymbol{V} = \frac{d}{d\varepsilon} j(\Omega_\varepsilon)\Big|_{\varepsilon=0}. \tag{29}$$

From (26), the derivative can also be written as:

$$Dj(\Omega) \cdot \boldsymbol{V} = D_1 J(\Omega, u(\Omega)) \cdot \boldsymbol{V} + D_2 J(\Omega, u(\Omega)) \cdot \dot{u} \tag{30}$$

where D_1 and D_2 denote the derivatives of J with respect to its first and second arguments respectively, and

$$\dot{u} = \frac{d}{d\varepsilon} u(\Omega_\varepsilon)\Big|_{\varepsilon=0} \tag{31}$$

is the derivative of the primal solution with respect to a change of the domain in the $\boldsymbol{V}$ direction.

The calculation in (30) has the drawback that in order to calculate the derivative of the functional, one has to calculate the derivative of the solution with respect to each direction of change of the domain Ω. While this calculation can be easily obtained by differentiating the variational form (18) in the $\boldsymbol{V}$ direction and then solving the corresponding problems for $\dot{u}$ (one for each possible direction), one asks the question whether the calculation of this term is indeed necessary in order to obtain the derivative of the functional $j(\Omega)$.

A method, called adjoint method in the sensitivity analysis literature, circumvents this problem mentioned above by introducing the solution of an

auxiliary problem, called the adjoint problem, and rewriting the expression for the derivative of $j(\Omega)$. We can arrive at this formulation using a method developed by Zolésio (1979), called the Lagrangian method for sensitivity calculations. For our case, we need to modify Zolésio's original method to account for expressions that evaluate to complex values. In the following, we briefly describe our modification of the original method.

We introduce the Lagrangian

$$\mathcal{L}(\Omega_\varepsilon, v_\varepsilon, \lambda_\varepsilon) = J(\Omega_\varepsilon, v_\varepsilon) + \mathrm{Re}(a(\Omega_\varepsilon; \lambda_\varepsilon, v_\varepsilon) - \ell(\Omega_\varepsilon; \lambda_\varepsilon)) \tag{32}$$

where $\mathrm{Re}(b)$ denotes the real part of a complex quantity b, and the scalar fields $v_\varepsilon \in \mathcal{S}_{\Omega_\varepsilon}$ and $\lambda_\varepsilon \in \mathcal{V}_{\Omega_\varepsilon}$. Using the mapping (27) we calculate:

$$\begin{aligned}\frac{d}{d\varepsilon}\mathcal{L}(\Omega_\varepsilon, v_\varepsilon, \lambda_\varepsilon) = {} & D_1 J(\Omega_\varepsilon, v_\varepsilon) \cdot \boldsymbol{V} \\ & + \mathrm{Re}(D_1 a(\Omega_\varepsilon; \lambda_\varepsilon, v_\varepsilon)) \cdot \boldsymbol{V} - \mathrm{Re}(D_1 \ell(\Omega_\varepsilon; \lambda_\varepsilon)) \cdot \boldsymbol{V} \\ & + \mathrm{Re}\big(a(\Omega_\varepsilon; \dot{\lambda}_\varepsilon, v_\varepsilon) - \ell(\Omega_\varepsilon; \dot{\lambda}_\varepsilon)\big) \\ & + \mathrm{Re}(a(\Omega_\varepsilon; \lambda_\varepsilon, \dot{v_\varepsilon})) + D_2 J(\Omega_\varepsilon, v_\varepsilon) \cdot \dot{v_\varepsilon}\end{aligned} \tag{33}$$

We now set $v_\varepsilon = u_\varepsilon$ where u_ε is the solution of the following variational problem: find $u_\varepsilon \in \mathcal{S}_{\Omega_\varepsilon}$ such that

$$a(\Omega_\varepsilon; w, u_\varepsilon) = \ell(\Omega_\varepsilon, w) \qquad \forall w \in \mathcal{V}_{\Omega_\varepsilon}. \tag{34}$$

We also set $\lambda_\varepsilon \in \mathcal{V}_{\Omega_\varepsilon}$ such that:

$$\mathrm{Re}(a^*(\Omega_\varepsilon; w, \lambda_\varepsilon)) + D_2 J(\Omega_\varepsilon, u_\varepsilon) \cdot w = 0 \qquad \forall w \in \mathcal{V}_{\Omega_\varepsilon}, \tag{35}$$

where $a^*(\Omega_\varepsilon; \cdot, \cdot)$ is the adjoint form of $a(\Omega_\varepsilon; \cdot, \cdot)$ defined as $a^*(\Omega_\varepsilon; \lambda_\varepsilon, u_\varepsilon) = a^*(\Omega_\varepsilon; u_\varepsilon \lambda_\varepsilon)$.

With this choice of the field v_ε we get:

$$\mathcal{L}(\Omega_\varepsilon, u_\varepsilon, \lambda_\varepsilon) = J(\Omega_\varepsilon, u_\varepsilon), \tag{36}$$

and by evaluating the derivative in (33) at $\varepsilon = 0$ we conclude:

$$\begin{aligned} Dj(\Omega) \cdot \boldsymbol{V} &= \frac{d}{d\varepsilon} J(\Omega_\varepsilon, u_\varepsilon)\bigg|_{\varepsilon=0} \\ &= D_1 J(\Omega, u) \cdot \boldsymbol{V} + \mathrm{Re}(a(\Omega; \lambda, u)) \cdot \boldsymbol{V} - \mathrm{Re}(D_1 \ell(\Omega; \lambda)) \cdot \boldsymbol{V}. \end{aligned} \tag{37}$$

Therefore, in order to evaluate the derivative of the functional $j(\Omega)$ we need to solve the state equation (18) and equation (35) at $\varepsilon = 0$. This will give us the primal field u and the adjoint field λ which we use to calculate the derivative in (37).

We now specialize the derivation above for the case where the functional $J(\Omega, u(\Omega))$ is given by:

$$J(\Omega, u(\Omega)) = \frac{1}{2}\int_{\Gamma_S} |u - u_d|^2 \, d\Gamma \tag{38}$$

where u_d is a given complex field with support on the surface $\Gamma_S \subset \Omega$.

We start by evaluating the terms in (35) for $\varepsilon = 0$:

$$D_2 J(\Omega, u) \cdot w = \mathrm{Re}\left(\int_{\Gamma_S} (u - u_d)^* w \, d\Gamma \right), \tag{39}$$

$$a^*(\Omega; w, \lambda) = (\nabla w, \nabla \lambda)^*_\Omega - k^2 (w, \lambda)^*_\Omega + (w, M^*(\lambda))^*_{\Gamma_R}, \tag{40}$$

where the operator M^* is given by:

$$M^*(\lambda) = (B(\lambda))^* + \sum_{n=N(d)}^{\infty} \sum_{j=-J(d)}^{J(d)} \hat{z}^*_{|n|}(k, R; d) \psi_{nj}(\boldsymbol{x}; d) \int_{\Gamma_R} \psi^*_{nj}(\boldsymbol{x}_0; d) \lambda(\boldsymbol{x}_0) \, d\Gamma_0. \tag{41}$$

So the field λ in (37) is chosen to be the solution of the variational problem: find $\lambda \in \mathcal{V}$ such that:

$$(\nabla w, \nabla \lambda)_\Omega - k^2 (w, \lambda)_\Omega - (w, M^*(\lambda))_{\Gamma_R} = -(w, u - u_d)_{\Gamma_S} \quad \forall w \in \mathcal{V}. \tag{42}$$

Finally, the derivative (37) is computed as follows:

$$Dj(\Omega) \cdot \boldsymbol{V} = G(u, \lambda, \boldsymbol{V}), \tag{43}$$

where

$$\begin{aligned} G(u, \lambda, \boldsymbol{V}) = \mathrm{Re} \Bigg\{ & \int_\Omega \left(\nabla \lambda^* \cdot \nabla u - k^2 \lambda^* u \right) \mathrm{div}\, \boldsymbol{V} \, d\Omega \\ & - \int_\Omega (\nabla \boldsymbol{V} + \nabla \boldsymbol{V}^T) \nabla \lambda^* \cdot \nabla u \, d\Omega \\ & + \int_\Omega \left(\lambda^* f \, \mathrm{div}\, \boldsymbol{V} + \lambda^* \nabla f \cdot \boldsymbol{V} \right) d\Omega \\ & + \int_{\Gamma_h} \lambda^* h \, (\mathrm{div}\, \boldsymbol{n}) \, \boldsymbol{V} \cdot \boldsymbol{n} \, d\Gamma + \int_{\Gamma_h} \lambda^* \nabla h \cdot \boldsymbol{V} \, d\Gamma \Bigg\}. \end{aligned} \tag{44}$$

Remark 1. In the adjoint method, we need to solve two variational problems, (18) and (42), to calculate the functional derivative. In these calculations there is no dependence on the direction $\boldsymbol{V}$ of change of the domain. As we will see, this has the important consequence that the cost of calculating the discrete approximation of the derivative does not depend on the number of parameters used to represent the domain.

Remark 2. It is interesting to find the boundary-value problem corresponding to (42). In this case, it is given by:

$$-\nabla^2\lambda - k^2\lambda = -(u - u_d)\,\delta(\boldsymbol{x} - \boldsymbol{x}_S) \quad \text{in } \Omega, \tag{45}$$

$$\lambda = 0 \quad \text{on } \Gamma_g, \tag{46}$$

$$\nabla\lambda \cdot \boldsymbol{n} = 0 \quad \text{on } \Gamma_h, \tag{47}$$

$$\nabla\lambda \cdot \boldsymbol{n} = M^*(\lambda) \quad \text{on } \Gamma_R, \tag{48}$$

where $\delta\ (\boldsymbol{x} - \boldsymbol{x}_S)$ is the Dirac measure in Γ_S. We can equivalently pose this problem in Ω_∞ as follows:

$$\nabla^2\lambda - k^2\lambda = -(u - u_d)\,\delta(\boldsymbol{x} - \boldsymbol{x}_S) \quad \text{in } \Omega_\infty, \tag{49}$$

$$\lambda = 0 \quad \text{on } \Gamma_g, \tag{50}$$

$$\nabla\lambda \cdot \boldsymbol{n} = 0 \quad \text{on } \Gamma_h, \tag{51}$$

$$\lim_{r\to\infty} r^{(d-1)/2}\left(\frac{\partial\lambda}{\partial r} + \mathrm{i}k\lambda\right) = 0. \tag{52}$$

From the above, we note that the appropriate boundary condition for the adjoint field λ at infinity is such that only incoming waves are allowed.

4. Numerical approximation

We now discuss the numerical approximation to the calculation of the shape derivative using the adjoint formulation developed above. We need to address each of the ingredients in the derivative calculation: the numerical calculation of the primal and dual solutions u and λ; the discretization of the domain Ω and the definition of the corresponding vector field $\boldsymbol{V}$; and the calculation of the derivative using (44).

We use the finite-element method to solve variational problems (18) and (42) for u and λ respectively. Particular attention needs to be given to the numerical implementation of the DtN and modified DtN boundary conditions and their counterparts in the adjoint formulation. In this work we use the approach developed by Oberai *et al.* (1998) where they present efficient algorithms for computing the matrix-vector products that are based on the outer-product structure of the DtN and the modified DtN maps. These algorithms are used in conjunction with the QMR algorithm (Freund and Nachtigal, 1991; Freund, 1992) to efficiently solve the resulting system of linear equations.

The boundary $\Gamma_B = \Gamma_g \cup \Gamma_h$ is discretized using quadratic B-splines, i.e. the boundary is parameterized using the following form (see Mortenson, 1997, chapter 5):

$$\boldsymbol{x}(u) = \sum_{i=0}^{n} N_{i,3}(u)\boldsymbol{x}_i \tag{53}$$

where $\boldsymbol{x}(u)$ is the position of a point in the boundary Γ_B, $n + 1$ is the number of control points of the quadratic B-spline, $N_{i,3}$ is the shape function corresponding to the ith control point $\boldsymbol{x}_i$, and u is a real number such that $0 \leq u \leq n - 1$. From the expression above the domain is uniquely characterized by $d(n + 1)$ parameters given by each of the d components of the $n + 1$ control points of the curve.

With this definition of the boundary description, we can define the vector field $\boldsymbol{V}$ on Γ_B as:

$$\begin{aligned} \boldsymbol{V}(\boldsymbol{x}(u)) &= \sum_{i=0}^{n}\sum_{k=1}^{d}\left(N_{i,3}(u)\boldsymbol{e}_k\right)V_{ik} \\ &= \sum_{i=0}^{n}\sum_{k=1}^{d}\boldsymbol{\Psi}_{ik}(u)V_{ik} \end{aligned} \tag{54}$$

where $\boldsymbol{e}_k$ is the kth unit vector in the Cartesian coordinate system. This defines a linear space for the set of admissible vector fields $\boldsymbol{V}$, where the basis is given by $\{\boldsymbol{\Psi}_{ik}(u) | i = 0, \cdots, n;\ k = 1, \cdots, d\}$. It is well-known that the domain derivative is uniquely determined by the definition of the normal component of $\boldsymbol{V}$ on Γ_B (see Sokolowski and Zolésio, 1992). Therefore, the derivative calculation is insensitive to the definition of $\boldsymbol{V}$ (and therefore its basis) in the interior of Ω. Since the calculation in (44) is performed in the interior of Ω, we need to choose an extension for the elements $\boldsymbol{\Psi}_{ik}$ over Ω. We choose this extension to be the solution of an auxiliary problem posed on a subset of Ω, which we denote Ω_{BL} (see Figure 2): find $\psi_i(\boldsymbol{x})$, $i = 0, \cdots, n$, such that:

$$\nabla^2\psi_i = 0 \quad \text{in } \Omega_{\mathrm{BL}}, \tag{55}$$

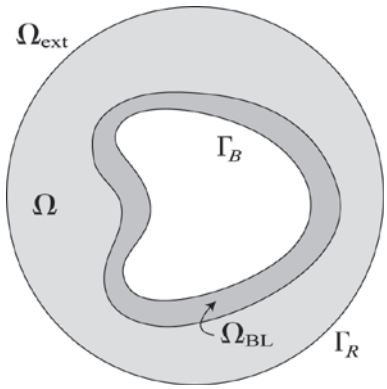

Figure 2.
Domain of definition for auxiliary problem (55)-(57)

$$\psi_i = N_i, 3 \quad \text{on } \Gamma_B, \tag{56}$$

$$\psi_i = 0 \quad \text{on } \partial\Omega_{\text{BL}} \setminus \Gamma_B. \tag{57}$$

Then, each element of the basis is given by $\boldsymbol{\Psi}_{ik}(\boldsymbol{x}) = \psi_i(\boldsymbol{x})\boldsymbol{e}_k$, $\boldsymbol{x} \in \Omega$. The finite element method is used to solve the $n + 1$ problems (55)-(57).

Remark 1. The subdomain Ω_{BL} is chosen to have only a small number of layers of finite elements in the vicinity of Γ_B. Therefore, the computation of the functions ψ_i is negligible when compared to the computation of the fields u and λ.

Finally, assuming u^h and λ^h to be the approximate solutions of the primal and adjoint problems respectively, we compute the approximation to the functional derivative as follows:

$$Dj(\Omega) \cdot \boldsymbol{V} = \sum_{i=0}^{n} \sum_{k=1}^{d} G(u^h, \lambda^h, \boldsymbol{\Psi}_{ik}) V_{ik}. \tag{58}$$

5. Numerical examples

In this section we present two numerical examples that use the procedure we have just described to calculate shape derivatives. The first example compares the accuracy of the calculation using (58) against analytical results. The second example is an inverse problem that is posed as an optimization problem. The latter is solved using a mathematical programming algorithm that requires calculation of the functional value and its gradient at each step. The adjoint method is used to calculate the gradient.

5.1 Example 1: pulsating cylinder

Consider the problem given by equations (1)–(4) where $f = 0$, $g = 1$, $k = 2.5$, $\Gamma_h = \emptyset$ and Γ_g is a circle of unit radius centered at the origin. We also consider the following shape functional:

$$j(\Omega) = \frac{1}{2} \int_{\Gamma_S} |u|^2 \, d\Gamma, \tag{59}$$

where the surface Γ_S is a fixed circle centered at the origin with radius $R_S = 5$. The surface Γ_g can be parameterized in terms of the coordinates of its center, (x_o, y_o), and its radius R_g. Therefore, the shape functional (59) depends on three parameters and its functional form can be written as follows:

$$j(\Omega) = j(x_o, y_o, R_g). \tag{60}$$

In this example we calculate the derivative of (59) with respect to each of the parameters x_o, y_o and R_g at $(x_o, y_o, R_g) = (0.0, 0.0, 1.0)$ using the adjoint method described in the last section. To solve the exterior Helmholtz problem and the adjoint problem we chose the DtN boundary (and also its counterpart in the

adjoint formulation) to be a circle of radius $R = 7$ centered at the origin (see Figure 3).

A Galerkin finite-element method is used to solve variational problems (18) and (42). Both problems were solved using the QMR iterative algorithm with the relative convergence tolerance set to 10^{-6}. We employed linear finite-elements (three-node triangles) in these calculations. Each of the problems (55)-(57) is solved on a small mesh comprised of a specified number of element layers around the curve Γ_g. Figure 4 shows the finite-element mesh used to calculate the derivatives shown in Table I for the case $h = 0.4$. The figure also shows the subdomain used for auxiliary problems which comprises five layers of elements (each layer is shown in a different tone of gray).

Table I compares the derivatives obtained using the adjoint formulation against analytical results for different values of the mesh size h. These results clearly show a good agreement with the exact solution for all derivatives. In order to compare these results with ones obtained using a different computational procedure, we provide in Table II the calculation of these

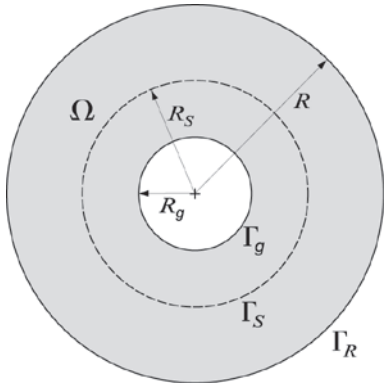

Figure 3.
Domain definitions for example 1

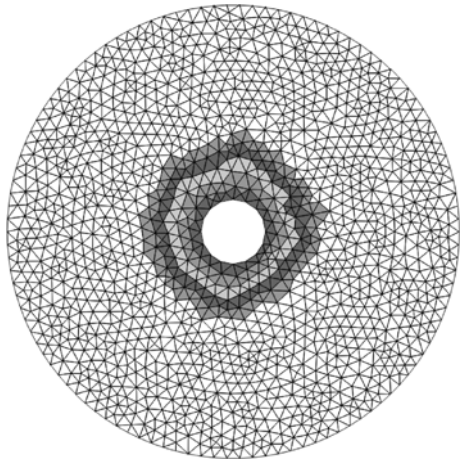

Figure 4.
Mesh used in the primal and adjoint calculations for the $h = 0.4$ case. The mesh consisting of five layers of elements used for the extension problem is shown in gray

derivatives using a central finite-difference approximation where the perturbation applied to each parameter equals the mesh size, i.e. the derivative (say, for example x_o) is approximated as follows:

$$\frac{\partial j}{\partial x_o}(x_o, y_o, R_g) \approx \frac{j(x_o + \Delta, y_o, R_g) - j(x_o - \Delta, y_o, R_g)}{2\Delta}, \qquad (61)$$

where $\Delta = h$. While a different choice of Δ could have been used, we found this one gives the best values. By comparing these two tables we conclude that the adjoint approach gives an approximation to the derivatives which is as accurate as the ones obtained using a finite-difference calculation. Moreover, the cost of computing these derivatives equals the cost of two exterior acoustics calculations: one for the primal problem, and one for the dual problem. For the finite-difference approximations, on the other hand, we need six exterior acoustics calculations.

Finally, one has to address the question of the stability of the adjoint calculation for different choices of the number of element layers (n) used in the extension problems (55)-(57). Table III shows the dependency on n is weak and therefore one should take n to be as small as possible. The choice $n = 1$ is particularly interesting for meshes consisting of three-node triangles since problems (55)-(57) are trivially solved in that case. (All the degrees of freedom in these problems are given prescribed data, and therefore, there is no problem to solve.)

		Adjoint calculation			
	Exact value	$h = 0.4$	$h = 0.2$	$h = 0.1$	$h = 0.05$
$\frac{\partial j}{\partial x_o}$	0.0	–3.632691e-002	2.506934e-002	1.709210e-003	7.590643e-004
$\frac{\partial j}{\partial y_o}$	0.0	2.384421e-003	–7.746614e-004	4.242509e-003	–9.965030e-004
$\frac{\partial j}{\partial R_o}$	3.099314e+000	2.887864e+000	3.034957e+000	3.125655e+000	3.109033e+000

Table I. Results using the adjoint method for different mesh sizes (h)

	Finite difference calculation			
	$h = 0.4$	$h = 0.2$	$h = 0.1$	$h = 0.05$
$\frac{\partial j}{\partial x_o}$	8.845458e-003	1.409610e-002	5.131970e-003	2.359672e-004
$\frac{\partial j}{\partial y_o}$	–3.532837e-002	–2.211589e-002	–2.717873e-003	4.785559e-003
$\frac{\partial j}{\partial R_g}$	2.979021e+000	2.978335e+000	3.072976e+000	3.092965e+000

Table II. Finite difference calculation of the derivatives for different mesh sizes. For all calculations we used $\Delta = h$

5.2 Example 2: an inverse problem

We are interested in obtaining the shape of an object immersed in an unbounded fluid medium from the knowledge of the pressure field on a surface enclosing it. We assume the wave-number for the problem is known, as well as the boundary condition imposed on the object's surface. Since such a problem may not admit a solution (Colton, 1984), we will instead find the shape of the object that minimizes the following functional:

$$j(\Omega) = \frac{1}{2}\int_{\Gamma_S} |u - u_T|^2 \, d\Gamma. \tag{62}$$

In (62), Γ_S is a closed surface where the target pressure field u_T is given.

This optimization problem is solved using a mathematical programming algorithm proposed by Herskovits (1991). This algorithm falls in the class of optimization algorithms known as interior point methods. A property of this class of methods is that the steps generated by the algorithm always lie within the feasible set for problems where the constraints on the variables are given by inequalities. The algorithm is given a starting point and generates a sequence of points that tend to a local minima of the functional. At each step, the algorithm requires the functional and its derivative, as well as the constraints and their derivatives in order to produce a new search direction. Within that direction, the algorithm looks for a local minima using an Armijo line-searching technique, which also requires the functional and its derivative at each step.

The problem we solved is shown in Figure 5. The wave-number for the acoustic calculations is $k = 2.5$ and a Dirichlet boundary condition with $g = 1$ is imposed on the surface of the body. No sources are present in the problem, so $f = 0$. The target pressure field in (62) is given by the solution of the exterior Helmholtz problem (1)-(4) where Γ_g is the "target" shape shown in the Figure. Γ_S is a circle centered at the origin with radius 5.0. In all the calculations we chose the DtN boundary as the circle centered at the origin with radius 7.0. In this problem we also set the relative tolerance of the QMR algorithm to be 10^{-6}.

We start the optimization algorithm with the "initial" shape shown in Figure 5. The algorithm stops when the shape functional attains 10^{-4} of its initial value. This curve is modeled using a quadratic B-spline with 16 control

Table III.
Effect of the number of layers used in the extension problem on the derivative calculation. Results shown are for the $h = 0.2$ mesh size

	Number of layers (n) used in the extension problem				
	$n = 1$	$n = 2$	$n = 3$	$n = 4$	$n = 5$
$\frac{\partial j}{\partial x_o}$	4.381172e-002	3.760443e-002	3.111201e-002	2.594314e-002	2.506934e-002
$\frac{\partial j}{\partial y_o}$	8.261661e-003	7.157206e-003	1.384386e-003	–1.079485e-003	–7.746614e-004
$\frac{\partial j}{\partial R_g}$	3.141090e-000	3.146896e+000	3.126735e+000	3.084069e+000	3.034957e+000

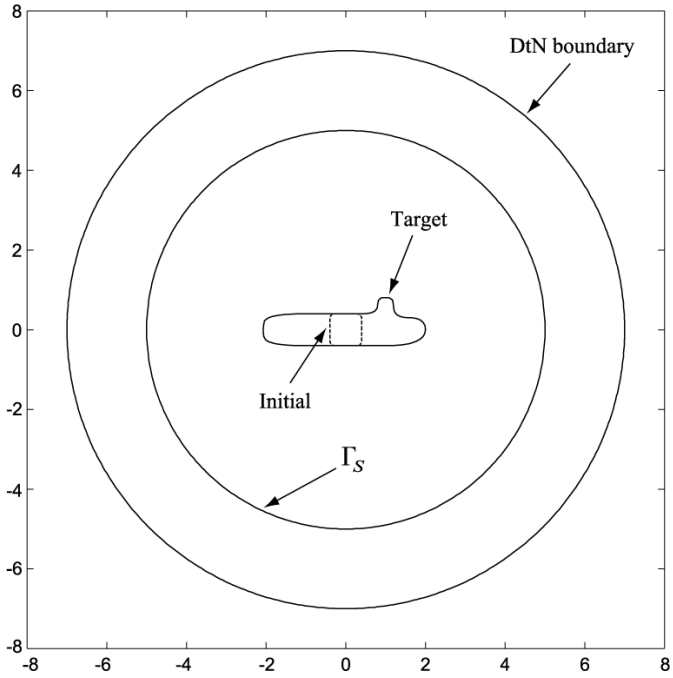

Figure 5.
Surfaces used in the inverse problem

points (which gives a total of 32 design variables for the optimization problem, one for each control point coordinate). A uniform finite-element mesh of size $h = 0.1$ was used in all calculations. A subdomain composed of five layers of elements around the object was used to solve for the extension problems (55)-(57). We imposed constraints on the variables such that all control points are contained in the box $\{(x, y) : -3 \leq x \leq 3, -3 \leq y \leq 3\}$. We also apply box constraints on the variables so that the B-spline is not allowed to cross itself. Figure 6 shows the initial shape and shapes corresponding to steps 13, 31 and 78 of the calculation. This figure shows that the curve corresponding to step 78 (which is the converged solution) is very close to the target shape. The overall procedure was able to get a very good approximation to the size of the object (both its length and width) and even the protrusion on its top-right side.

Figure 7 shows the convergence history of the optimization algorithm. A step in the calculation amounts to a functional evaluation and calculation of its derivatives. Therefore, the total number of problems solved until convergence is 156. This compares to a total of 2,496 calculations which would be needed if a finite-difference scheme was used to calculate the derivatives. The total time required to solve all the extension problems is about 5 percent of the time for an acoustic calculation.

6. Conclusions

The problem of computing derivatives of shape functionals with constraints given by the scalar Helmholtz equation posed on an unbounded domain has

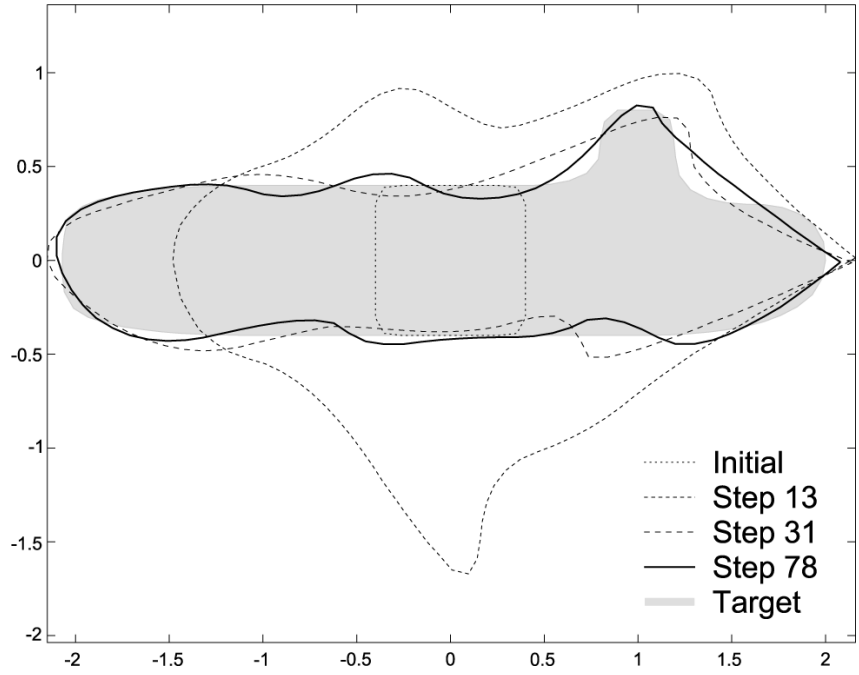

Figure 6.
Evolution of the surface during three steps of the calculation. Initial and target shapes are also shown

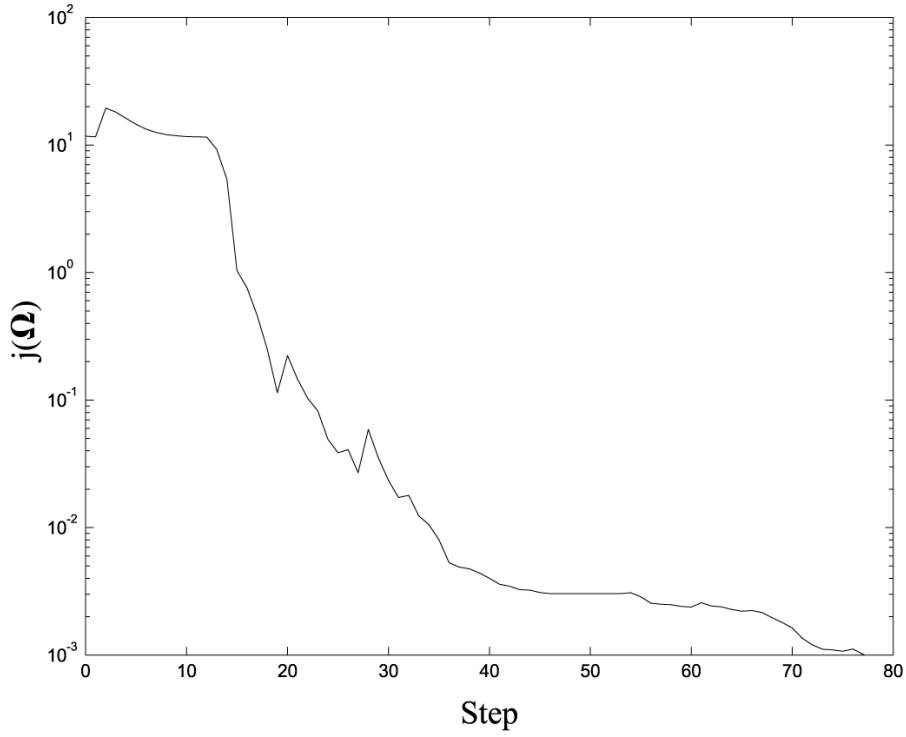

Figure 7.
Convergence history of example 2

been investigated. We have proposed an extension of the Lagrangian method in sensitivity analysis so that it can be used in problems where the primal field is a complex field. This allows us to obtain the adjoint equations corresponding to these problems. The solution of the primal and the adjoint problem obtained through this technique allows us to calculate the derivative of the shape functional for any change in shape. Numerical examples presented in this work show the good accuracy attained in the calculation of these derivatives as well as the gains in speed when compared to other numerical procedures.

References

Colton, D. (1984), "The inverse scattering problem for time-harmonic acoustic waves", *SIAM Review*, Vol. 26 No. 3, July, pp. 323-50.

Freund, R.W. (1992), "Conjugate gradient-type methods for linear systems with complex symmetric coefficient matrices", *SIAM J. Sci. Statistic. Comput.*, Vol. 1 No. 13, pp. 425-48.

Freund, R.W. and Nachtigal, N.M. (1991), "QMR: a quasi-minimal residual method of non-hermitian linear systems", *Numer. Maths.*, Vol. 1 No. 60, pp. 315-39.

Hadamard, J. (1968), *Mémoire sur un problème d'analyse relatif a l'équilibre des plaques élastiques encastrees*, Mémoire des savants etrangers, Ouvres de J. Hadamard, CNRS, Paris.

Herskovits, J.N. (1991), "An interior point method for nonlinear constrained optimization", in Rozvany, G. (Ed.), *Optimization of Large Structural Systems*, Vol. 1, NATO/ASI series, Springer-Verlag, Berlin, pp. 589-608.

Keller, J.B. and Givoli, D. (1989), "Exact non-reflecting boundary conditions", *Journal of Computational Physics*, Vol. 82 No. 1, pp. 172-92.

Mortenson, M.E. (1997), *Geometric Modeling*, 2nd ed., John Wiley & Sons, Inc., New York, NY.

Oberai, A.A., Malhotra, M. and Pinsky, P.M. (1998), "On the implementation of the Dirichlet-to-Neumann radiation condition for iterative solution of the Helmholtz equation, *Applied Numerical Mathematics*, Vol. 27, pp. 443-64.

Sokolowski, J. and Zolésio, J.-P. (1992), "Introduction to shape optimization: shape sensitivity analysis", *Springer Series in Computational Mathematics*, Vol. 16, Springer-Verlag, Berlin.

Zolésio, J.-P. (1979), "Identification de domains par déformations", Thèse d'etat, Université de Nice.